Contents lists available at ScienceDirect

Journal of Energy Storage

Research papers

Guide for the development and evaluation of supercapacitors with the proposal of a novel design to improve their performance

Jesús M. Rodríguez-Rego [a], Juan Pablo Carrasco-Amador [a], Laura Mendoza-Cerezo [a], Alfonso C. Marcos-Romero [a], Antonio Macías-García [b,*]

[a] Departamento de Ingeniería Mecánica, Energética y de Materiales, Escuela Técnica Superior de Ingenieros Industriales, Universidad de Extremadura, Avenida de Elvas, s/n., 06006 Badajoz, España
[b] Departamento de Expresión Gráfica, Escuela Técnica Superior de Ingenieros Industriales, Universidad de Extremadura, Avenida de Elvas, s/n., 06006 Badajoz, España

ABSTRACT

Supercapacitors, as an energy storage device, have shown great potential as a tool to help solve today's energy problems. There are currently three types of supercapacitors: electrochemical double layer, pseudocapacitors and hybrid supercapacitors. They have aroused great interest due to their high-power density, fast charging and discharging and good cyclic behaviour, and nowadays, it is necessary to continue their study in order to extend their capabilities. This work proposes a design and fabrication method for supercapacitors with a materials guide that, firstly, guides researchers in the development of supercapacitors and, secondly, proposes an improvement of the current supercapacitor design to ensure parallelism of the collectors, avoid corrosive processes of the collectors using graphite and avoid pad breakage. All this is carried out with 3D design and additive manufacturing or 3D printing technologies, which means a reproducible solution with low available resources. In addition, the model proposed here avoids the breakage of the pads that act as electrodes by designing an intermediate body that prevents the Swagelok® cell thread from being consumed.

1. Introduction

Global energy consumption is steadily increasing, driven both by the socio-economic growth of nations and by the increase in the world's population, which will reach 9.1 billion in 2050 [1]. Part of the energy demand comes from fossil fuels, which produce 80 % of the world's primary energy and whose abundant global reserves will continue to be used for many years to come. However, there is a limit to environmental protection and care in the face of the threat of global warming [2], which is caused by greenhouse gases generated during the use of these fuels in the energy production process. For this reason, there is a worldwide declaration of interest in limiting them, such as the European Commission's 20/20/20 Plan, whose objectives are to reduce greenhouse gas emissions from the combustion of fossil fuels by 20 % [3].

One possible solution to the major environmental problem associated with energy production would be to implement the use of clean and renewable energies. Generally speaking, electrical energy can be easily generated, transported and transformed, but it presents the difficulty of storing it in large quantities. In addition, the problem facing the use of

renewable energies is that they are highly dependent on various climatic factors, so that their energy production efficiency may suffer discontinuities and may not be sufficient to meet society's energy needs. For this reason, it is of great importance to research and develop energy storage devices that allow a balance between energy demand, generation from renewable sources and increasing storage capacity to ensure electricity consumption [4,5] (Fig. 1).

Based on the above, the objective of this work is to investigate the improvement of existing technologies that favour more efficient energy storage. Within the diversity of existing energy storage systems (batteries, fuel cells, capacitors and supercapacitors), the design, study and improvement of supercapacitors are of great interest [6].

The construction of better energy storage devices is not only based on the material properties of electrodes and electrolytes, but also depends significantly on the configuration of the devices [7–9].

Therefore, a methodology is proposed that improves the characterisation process of the materials used in the manufacture of the electrodes, selecting which of them could be the most suitable for their manufacture. In this way, an optimisation of the material used and
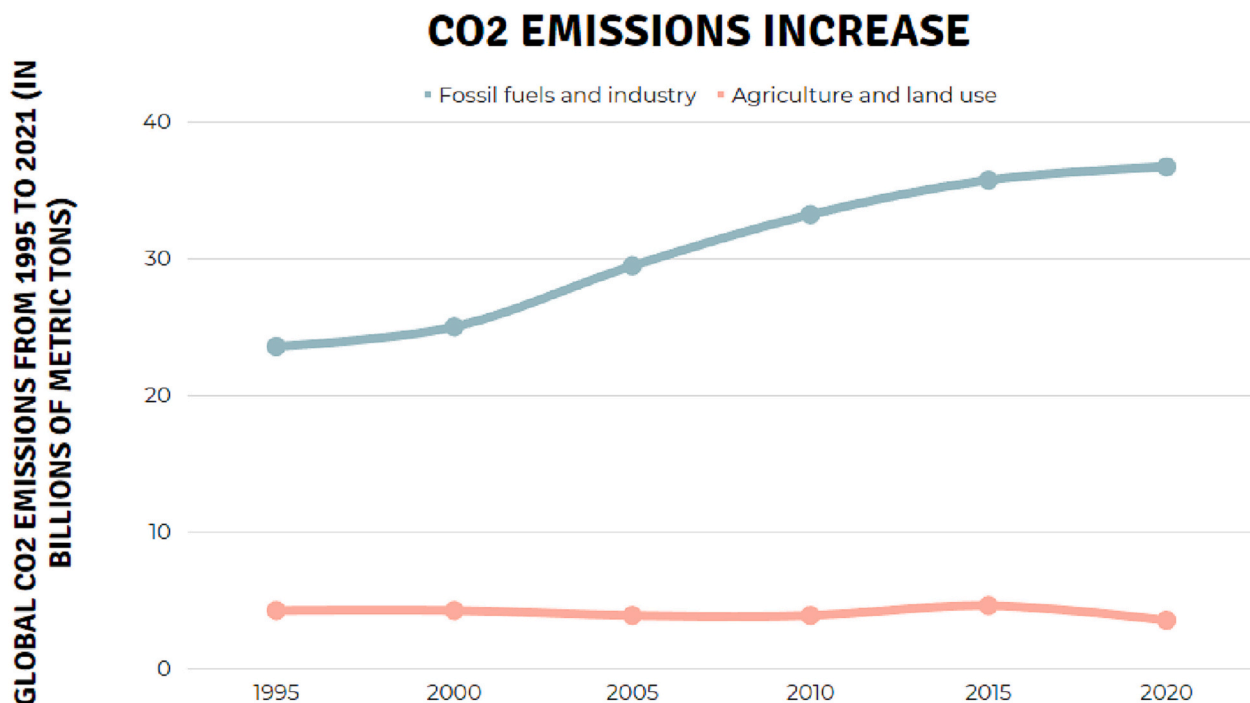

CO2 EMISSIONS INCREASE

Fig. 1. Increase in CO_2 emissions. The graph shows the global CO_2 emissions from 1995 to 2020, where we can clearly see the increase of these emissions every year in a linear way [45].
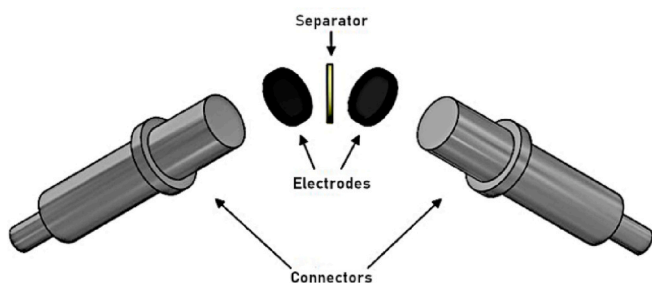

Fig. 2. Main elements of a supercapacitor excluding the body that supports the other elements shown (connectors, electrodes and separator).

studied is achieved, and the results obtained are improved.

In addition, a possible solution to one of the most common problems during the assembly of a Swagelok® cell is indicated, which is the breakage of the activated carbon discs (electrodes) due to the fact that there is no system to stop the number of turns that can be made when screwing the moving parts of the device, which often causes the fragmentation of the activated carbon discs due to the overpressure that they are subjected to. This problem invalidates the test carried out, and makes it necessary to carry out the device preparation procedure again. Therefore, by means of computerised design, the creation of a new intermediate body with an optimal height to limit the thread and thus avoid the breakage of the electrodes is proposed. Subsequently, the design of each of the parts that make up this new cell is described.

In this way, the work gathers the necessary information to facilitate the learning process for the manufacture of supercapacitors, as well as their validation. In addition, it proposes a new mechanical design of the components that form it, and provides the tools to characterise the electrodes, achieving a reproducible and improved design of supercapacitors.

2. Materials and method

2.1. Methodology

3D design applied to the improvement of energy storage systems opens a new avenue of research in the improvement and manufacture of this type of system. To do this, firstly, we will develop a new design with Autodesk Inventor® that includes both improvements to existing designs and new improvements.

Secondly, we will proceed to the fused deposition modelling process (3D printing) which will be the method for manufacturing the designs made with Autodesk Inventor®.

To make the supercapacitor proposed in this study, the following software and equipment have been used to manufacture the body of the supercapacitor formed by the collectors and the Swagelok® cell, regardless of the material used to make the rest of the components such as the electrodes, separator, and electrolyte (Fig. 2).

➢ Equipment:
   o Ender 3 pro 3D printer. Low cost FDM printer [10].
   o Autolab PGSTAT204. The potentiostat allows the possibility of controlling and measuring the potential of the cell, detecting changes in its resistance, and varying the intensity of the current administered to the system, keeping the potential difference constant. It is an application of Ohm's law [11].

➢ Software:
   o Ultimaker Cura. Application designed for 3D printers, which allows to modify printing parameters and transform the modified file to G-code [12].

o Autodesk Inventor. Autodesk Inventor is a 3D parametric solid modelling package produced by the software company Autodesk [13]. It competes with other computer-aided design software such as SolidWorks, Pro/ENGINEER, CATIA and Solid Edge. Autodesk Inventor is based on parametric modelling techniques. Users begin by designing parts that can be combined into assemblies. By correcting

Table 1

Categories of additive manufacturing as defined by the ASMT [16].

Category	Description
Binder jetting	A bonding agent is selectively deposited to bind the powder
Material jetting	Small particles of material are deposited in a selective manner
Powder bed fusión	Energy source selectively melts regions of powdered material
Directed energy deposition	An energy source melts the material as it is deposited
Sheet lamination	Different layers of material are deposited in a molten state
Vat photopolymerymerization	A liquid photopolymer is cured by a light bulb
Material extrusion	A material is selectively dispensed and disposed on a surface through an injector

parts and assemblies, several variants can be obtained [14]. Inventor uses specific file formats for parts (.IPT), assemblies (.IAM), drawing view (.IDW and .DWG) and presentations (IPN). The latest versions of Inventor include numerous enhancements such as Shape Manager, tools for creating plastic parts and their respective injection moulds, finite element stress analysis and dynamic analysis, creation and analysis of structures, piping, and wiring, iPart, iAssembly, iMates, iCopy, iLogic etc. technologies.

o Autocad. Computer-aided design software 3D printing [15].

o NOVA software. It allows different types of electrochemical analysis using a Potentiostat/Galvanostat. In this work, its use is mainly proposed to perform analysis using the cyclic vontammetry technique and charge-discharge analysis of the supercapacitor.

Additive manufacturing processes all start from a 3D computer-designed model, usually with an STL (STereo Lithography) extension. This file can also be extracted from a 3D scanner, which favours the reproduction of parts. The STL file contains the geometric information of the part represented in a simple mesh. This file is then "sliced" into discrete 2D layers for printing.

Different technologies are available on the market to produce a part by 3D printing. In this study we will follow the classification offered by the ASTM (American Society for testing and Materials) and we will separate the different technologies into 7 different typologies as shown in Table 1 [16].

In our work we will focus on the printing system based on the extrusion of the material through a nozzle.

2.2. Supercapacitors, electrochemical capacitors, or double layer capacitors (EDLCs)

Supercapacitors are devices for storing electrical energy in the form of electrostatic charges confined in small devices, consisting of pairs of conductive plates separated by a dielectric medium.

This technological leap towards supercapacitors comes from something as simple as increasing the specific surface area of the electrodes and bringing the charges of opposite sign closer to molecular size. By using materials with a high specific surface area, such as activated carbons, it is possible to obtain 100,000 times higher specific surface area values than with a smooth material with a much lower weight per area. Capacitances around 1 million times higher than those of a conventional capacitor of similar size and weight can be achieved.

Their construction is like that of batteries, where there are two electrodes immersed in an electrolyte. The two electrodes are separated by a semi-permeable material that prevents a short-circuit between the electrodes but allows ions from the electrolyte material to pass through. When a potential difference is applied, a charge density gradient is created between the plates and the ions migrate towards the electrode
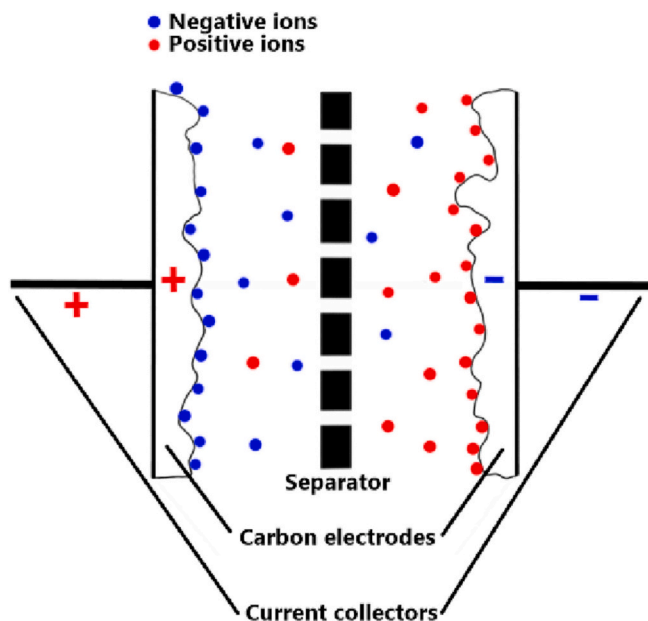

Fig. 3. Schematic of a charged double-layer capacitor (EDLC) (own elaboration) [46].
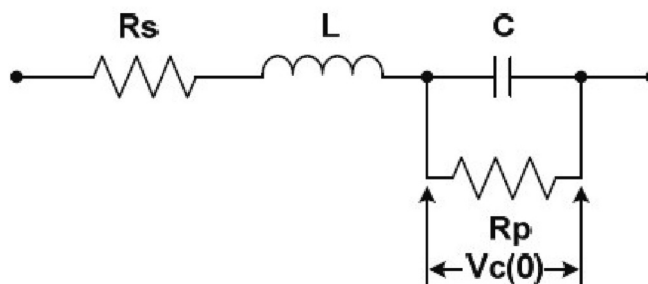

Fig. 4. Electric circuit equivalent to a supercapacitor.

surface and adsorb on the interfacial region. In such a device, each electrode-electrolyte interface represents a capacitor, so that the complete cell can be considered as two capacitors in series (Fig. 3) [17].

Supercapacitors are characterised by the fact that they can be charged and discharged in very short periods of time, in the order of a second or even less, which makes them particularly suitable for peak power requirements or short-term power interruptions. This is because the charge storage is purely electrostatic.

The term supercapacitor encompasses different types depending on the type of electrode used, operating principle or design. There are many classifications, but one of the most widely accepted encompasses 3 types of supercapacitors: EDLCs (Electrochemical Double Layer Capacitors), pseudocapacitors and hybrid supercapacitors [18].

Fig. 4 shows the equivalent circuit.

This scheme consists of a capacitor (C), a parallel leakage resistor (Rp), which models the energy loss due to self-discharge of the capacitor; an Equivalent Series Resistor (ESR) (RS), which models its losses in the charging and discharging processes; and a series coil (L) which completes the dynamic model of the capacitor. In a supercapacitor Rp is always much higher than Rs.

For the development of this work, we are going to use a Swagelok® type electrochemical cell in a two-electrode configuration, whose scheme is shown in Fig. 5.

The capacitance can be found in the same way as for a conventional capacitor, Eq. (1).
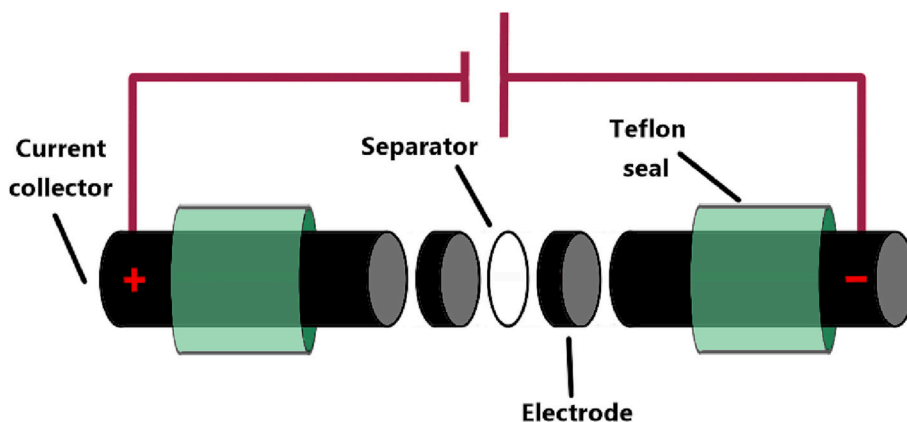
Fig. 5. Schematic diagram of an electrochemical cell in two-electrode configuration (own elaboration).

$$C = \frac{q}{V} = \frac{q}{\frac{q \cdot d}{\varepsilon \cdot A}} = \frac{\varepsilon \cdot A}{d} \tag{1}$$

where: q: ratio of the maximum charge that can be stored in a capacitor to the maximum charge that can be stored in a capacitor. V: voltage applied across its plates. ε: dielectric material constant. A: area of the plates. d: separation distance.

The energy and maximum power of supercapacitors are obtained from the following Eqs. (2) and (3) respectively:

$$W = \frac{1}{2} \cdot C \cdot V^2 \tag{2}$$

$$P_{max} = \frac{W^2}{t_d} \tag{3}$$

where: V: nominal potential. t_d: time taken for the discharge of the supercapacitor.

➤ EDLSs: electrical double layer capacitors

In this type of supercapacitor, the energy is stored through the formation of a double layer at the electrolyte/electrode interface.

Therefore, the supercapacitor consists of two capacitors in series, each of them forming at the electrolyte/electrode interface.

If we denote the capacitance of these two capacitors as C_1 and C_2, the capacitance of the supercapacitor, C, will be [18]:

$$\frac{1}{C} = \frac{1}{C_1} + \frac{1}{C_2} \tag{4}$$

The EDLC mechanism requires electrodes made of high specific surface area materials, which increase the charge accumulation capacity, and a convenient pore structure that allows rapid movement of the electrolyte ions, which is achieved by constructing the electrodes with carbonaceous materials.

➤ Pseudocapacitive supercapacitors

In the case of pseudocapacitors, energy is stored through reversible oxidation-reduction (redox) reactions, which involve the transfer of electrons associated with reversible changes in the oxidation state of one of the atoms or molecules that constitute the active electrode material. These faradaic-type redox reactions result in the accumulation of electrical charge in a manner like that occurring in a battery [18,19].

The capacities associated with a pseudocapacitive mechanism can be up to 10 times higher than the capacities due to a double layer mechanism because in addition to the formation of the electrical double layer, the development of redox reactions, whose rate of charge transfer is dependent on the operating voltage of the system, contributes positively to the energy storage. This phenomenon is known as pseudocapacitance [20].

The origin of these pseudocapacitive contributions can be the presence of active functional groups on the surface of the electrode material [21], the nature of the material itself which, as in the case of transition metal oxides [22] or conductive polymers [23] undergo redox reactions under the working conditions of the system, or the development of hydrogen electroadsorption and/or ionic intercalation processes at the electrodes [24].

➤ Hybrid supercapacitors

Hybrid supercapacitors seek to harness the advantages of EDLCs and pseudocapacitors and minimise their disadvantages to obtain better performance by pairing two different electrodes with different charge storage mechanisms to deliver high energy without sacrificing power
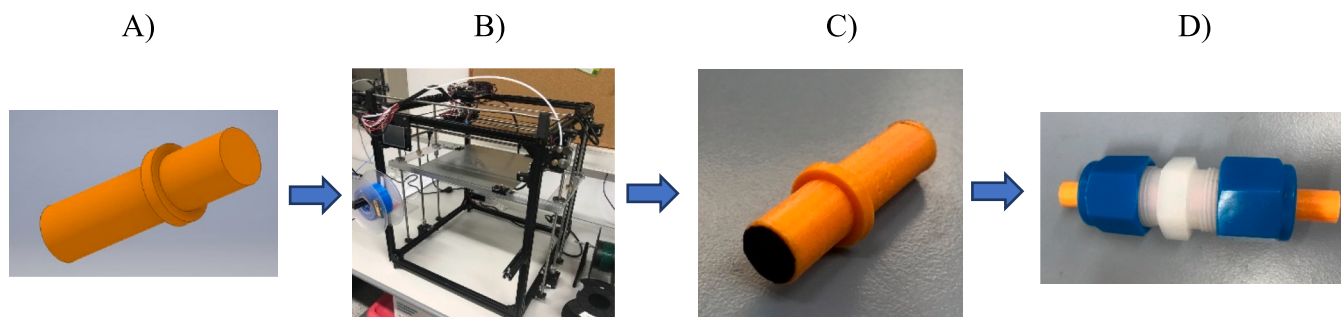
A)   B)   C)   D)

Fig. 6. Manufacturing process of the supercapacitor prototype and parallelism check. Image A) shows the pre-design of a collector in Inventor; Image B) shows the 3D printer with the g-code file to be executed; Image C) shows the collector with a tinted face; Image D) shows the result of the connectors attached to the Swagelok® cell.
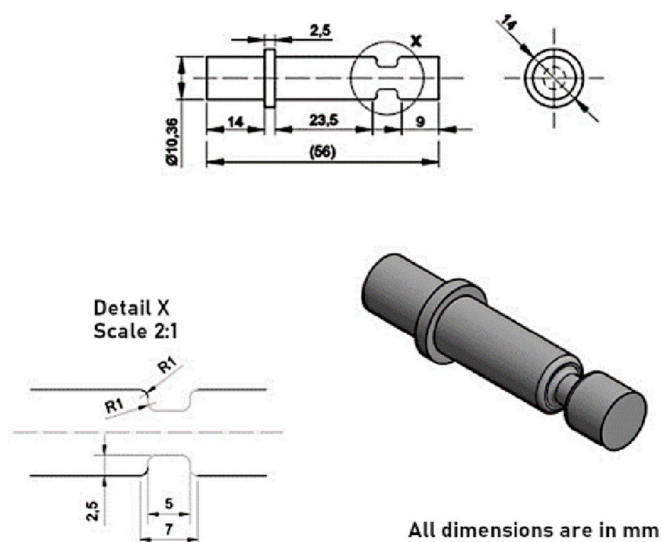
Fig. 7. Autocad drawing of the connector made of graphite so that it can be manufactured in any company or parts machining laboratory.

output [25].

In these supercapacitors, the energy mechanisms presented by each of the electrodes that make up the device are of a different nature [26]. One electrode acts as a support for the redox reactions, presenting a battery-type electrochemical behaviour, while the other presents a capacitive-type storage mechanism (capacitor-type electrode) [27].

The charge storage capacity of the capacitor electrode limits the energy stored in the system, and thus the cell capacity (C) and/or the specific electrode capacity (C_{el}) [26].

3. Results and discussion

3.1. Design and printing of connectors

Firstly, some PLA connectors were designed and printed to check the assembly and parallelism of these connectors inside the Swagelok® cell in a simple, quick, and economical way.

In this way, if one side of the connector is dyed and when the connectors are assembled inside the Swagelok® cell, the entire side of the other connector is uniformly dyed, the parallelism is correct (Fig. 6).

After checking that the parallelism was correct and that the number of contact points between the two connectors is high, it was necessary to model and machine a connector from a material that would not undergo aggressive oxidation processes or galvanic couples. For this reason, and after carrying out tests on copper, which gave poor results, it was decided to manufacture in graphite (Fig. 7).

3.2. Electrode fabrication and electrolyte selection

Electrode materials can be classified into three main groups [28]:

➢ Carbon materials
➢ Conductive polymers
➢ Metal oxides

In order to make the right choice of starting materials for the manufacture of electrodes, a characterisation is proposed that includes:

➢ Textural characterisation by N2 adsorption at 77 K and mercury porosimetry using an Autosorb-1, Quantachrome and an Autoscan-60 respectively. The 77 K N2 adsorption technique allows the determination of the specific surface area and the volume of
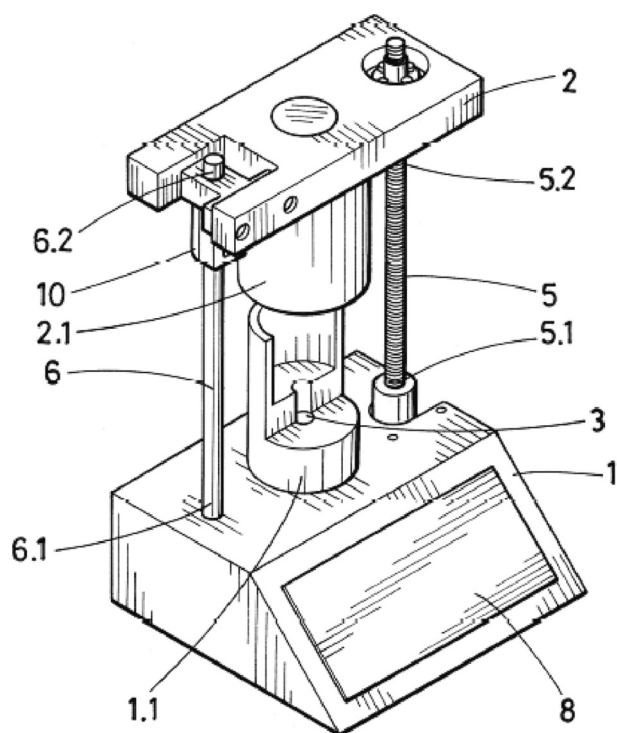

Fig. 8. Electrical conductivity measuring equipment for powdery, carbonaceous, or granular materials (P202130647). It allows the electrical conductivity of powdery materials to be measured under certain conditions of applied humidity and pressure. Subsequently, by means of an algorithm, it can predict the conductivity of the material to be studied under other pressures or, in other words, under other particle separation distances.

micropores and narrow mesopores, while mercury porosimetry determines the volume of wide mesopores and macropores.
➢ Determination of electrical conductivity using the device developed and patented by the Materials Engineering research group of the University of Extremadura entitled "Electrical conductivity measuring equipment for powdery materials", which can be found on the website of the Spanish Patent and Trademark Office with application number "P202130647" (Fig. 8).

In this work we will focus mainly on the use of carbon materials, due to their high capacity to make use of waste and therefore to recycle materials.

3.2.1. Manufacturing carbon materials from recycled material

The use of techniques and equipment to produce activated carbon from waste products (cherry stones, coffee endocarp, chestnut wood residues, vine shoots, olive wood, chestnut shells, etc.) has been extensively studied and the results shown in the articles are that the activated carbon obtained has multiple uses.

In recent years, adsorption systems involving activated carbon have gained importance in purification and separation processes on an industrial scale. The characteristics of activated carbon depend on the physical and chemical properties of the precursor, as well as on the method of activation [29].

There are two methods for preparing activated carbons:

➢ Physical activation. Comprising two steps: a carbonisation step and an activation step.
➢ Chemical activation. A raw material is impregnated with an activating reagent and the impregnated material is heated in an inert atmosphere. In the literature, several studies using $ZnCL_2$ [30], they achieve a maximisation of the adsorption capacity and bulk density
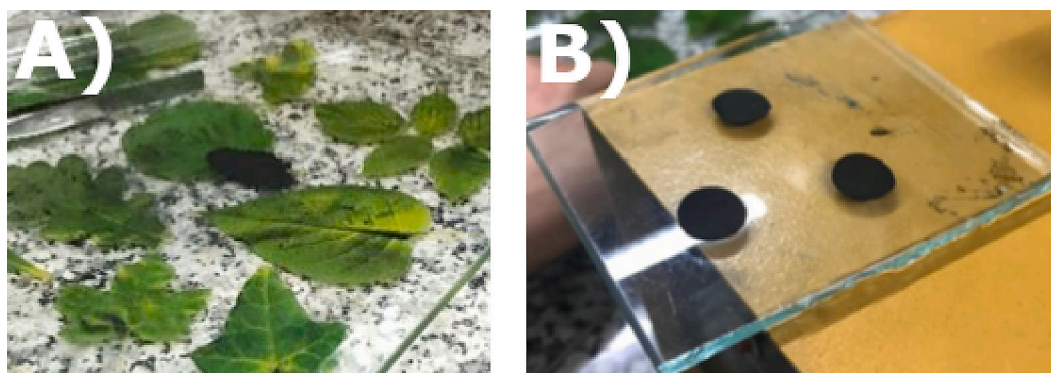
Fig. 9. A) Homogeneous stretched mass of material. It is critical that there are no pores/cavities or significant evidence of different thicknesses in the mass, resulting in poor homogeneity. B) Electrodes resulting from the proposed method for preparing electrodes. A good result of shape and homogeneity is observed.

of activated carbons produced from cellulosic and lignocellulosic materials. However, more work is found where phosphoric acid is used due to the corrosion problems, inefficient chemical recovery and environmental disadvantages associated with zinc chloride [31]. This reagent induces important changes in the pyrolytic decomposition of the lignocellulosic materials, promoting depolymerisation, dehydration and redistribution of the constituent biopolymers [32], favouring the conversion of aliphatic to aromatic compounds at lower temperatures than heating in the absence of additive, thus increasing the yield.

The advantage of chemical activation over physical activation is that it is carried out in a single step and at relatively low temperatures. Typically, ≤ 500 °C for wood activation with phosphoric acid [33] and between 600 and 700 °C for the activation of lignocellulosic materials impregnated with $ZnCl_2$ [34].

However, the most important disadvantage of chemical activation is the incorporation of impurities from the activating agent.

3.2.2. Electrode preparation

The proposed method of preparing the electrodes consists of:

➤ Grind the materials to be used and prepare a mixture of the starting material with polytetrafluoroethylene and ethanol and, using a heated magnetic plate, mix and heat until the ethanol evaporates.
➤ The resulting paste is stretched and moulded to the desired dimensions on a glass plate with controlled addition of stanol until a homogeneous stretched mass of material is obtained (Fig. 9A).
➤ Then, after checking that the stretched mass has no pores, we obtain the circular electrodes by means of a 7 mm punch. The electrodes obtained are placed between two sample holders and placed in an oven at 100 °C for 12 h (Fig. 9B).

On the other hand, the selection of the separator and electrolyte is necessary to manufacture a supercapacitor [18], because the performance of a supercapacitor is affected by both the materials of the electrodes and the electrolytes used. The electrochemical stability of the electrolytes is critical in determining the operating voltage and lifetime of supercapacitors. In aqueous supercapacitors with Zn film electrodes,
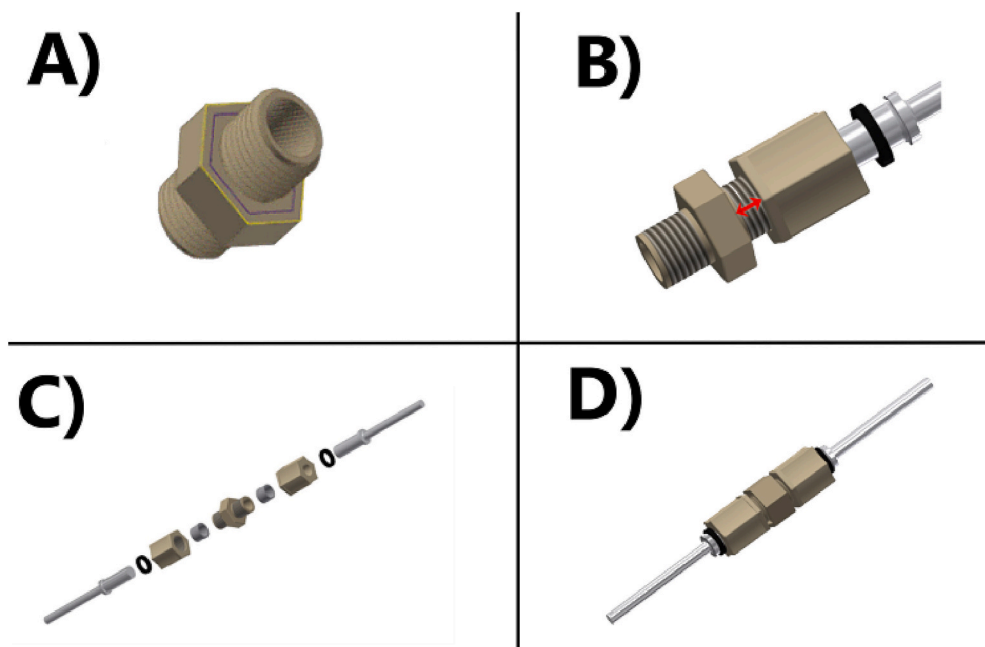

Fig. 10. A) Autodesk Inventor design of the intermediate body perimeter. B) Distance to be measured in the tests to adjust the body to ensure the integrity of the electrodes inside the body. C) Virtual mock-up of the Swagelok® cell designed with all the elements that make up the supercapacitor body. D) Swagelok® cell developed in this work that reduces the chances of electrode breakage due to overpressure caused by poor fit of the collectors inside the supercapacitor body.

Table 2
Measurements made in the tests.

Assay	Distance (mm)	Pad breakage
1	1.9	No
2	1.5	Yes
3	2	No
4	2.1	No
5	2.2	No
6	1.4	Yes
Mean	2.05	

strong alkaline electrolytes, such as KOH solution, are not suitable due to the formation of ZnO, which is detrimental to the cyclability of the cell. Meanwhile, strongly acidic electrolytes, such as H_2SO_4, can react with the Zn metal to generate H_2 [35].

➢ Separator: Usually a membrane made of an inert, porous material that allows the movement of the electrolyte ions and prevents contact between the two electrodes.
➢ Electrolyte: A liquid that provides ions to form the electrochemical double layer so that energy can be stored and released. In some cases, the ions in the electrolyte can interact with the electrode surface through redox reactions. This mechanism of energy accumulation and release is called a pseudocapacitive mechanism.
   o Aqueous electrolyte: They have a high ionic conductivity, in the order of 1 S/cm, and a low working voltage. [36].
   o Organic electrolytes: These are composed of organic salts dissolved in organic solvents. The ionic conductivity is of the order of 0.1 S/cm [37] and they can reach a working voltage of 2.5–2.7 V, which allows the energy density to be increased. Their capacity is due to a double layer mechanism.
   o Ionic liquid type electrolyte: These are organic salts that are molten at room temperature and therefore do not have a solvent. The ionic conductivity is low, in the order of 0.001 S/cm and a working voltage can reach 3.5 V which increases the charge density. The capacity of these electrolytes is mainly due to a double layer mechanism.

3.3. Virtual design of the Swagelok® cell and assembly of the supercapacitor

One of the most common problems with the assembly of the Swagelok® cell is the breakage of the activated carbon discs (electrodes), due to the fact that there is no system to stop the number of turns that can be made when threading the moving parts of the device, which often causes the carbon discs to fragment due to the overpressure supported by an excess of thread, thus rendering the test invalid and causing the whole procedure to be repeated, resulting in a great loss of time.

The design of the Swagelok® cell using parametric drawing software allows different solutions to be tested virtually, saving the manufacture of parts that do not prove to be valid in the end. To obtain a virtual model of the Swagelok® cell using Autodesk Inventor, the following methodology has been devised:

➢ Create a project in Autodesk Inventor®, so that all the elements created are stored in the same directory.
➢ Take the original Swagelok® cell and make a sketch of all its measurements.
➢ The Swagelok® cell is made up of the following elements: 2 current collectors (originally made of steel, although in this work it is proposed to make it out of graphite), 1 intermediate body, 2 threaded elements, 2 self-locking washers and 2 gaskets to prevent the fluid from escaping from the cell (Fig. 10C).

To solve the problem of electrode placement, a new intermediate body was designed to limit the thread and avoid breakage of the activated carbon tablets due to over-threading of the device. For this purpose, an intermediate body was designed with an optimum height that never allows the thread to be used up until the entire thread is consumed.

To determine this height (Fig. 10B), it was necessary to use a caliper gauge to measure the distance between the bottom face of the element being threaded into the intermediate body and the top face of the hexagonal washer of the intermediate body. Tests where the distance that prevented breakage of the carbon electrode was considered valid, while
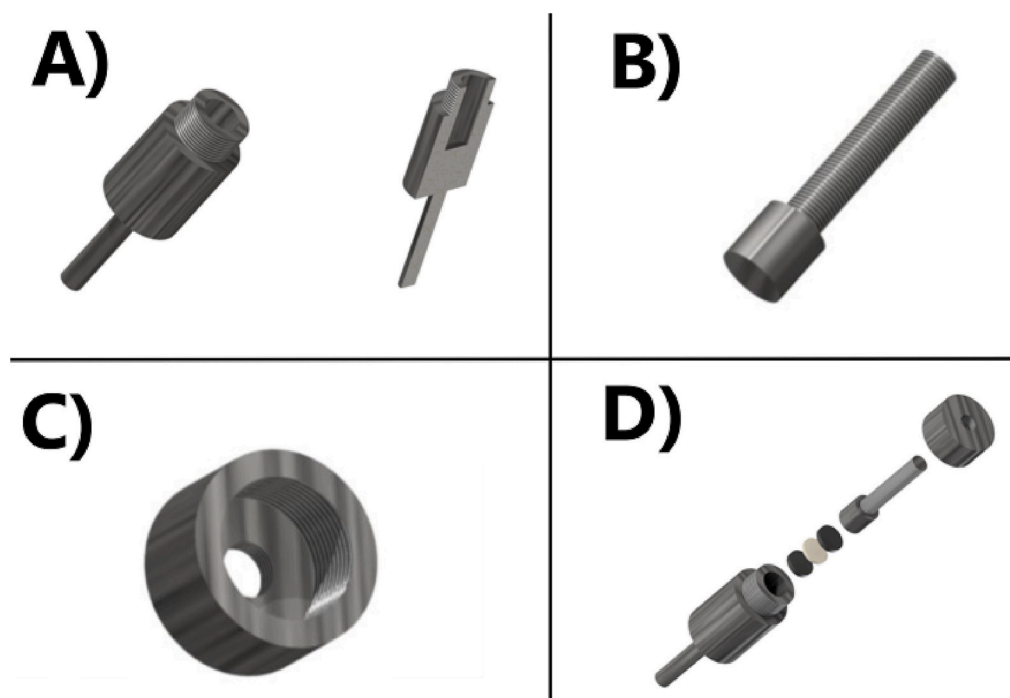

Fig. 11. A) Fixed body of the new electrochemical cell and cross-section of the cell. B) New mobile threaded manifold. C) System locking device. D) Exploded system detailing the position of the electrodes in black and the separator in white.

Fig. 12. Final result of the body inserted in the newly designed Swagelok® cell. An improvement in the design for the manufacture of supercapacitors is achieved by ensuring parallelism and the correct connection of the elements that make up the supercapacitor without jeopardising its structural integrity.

the distance that resulted in breakage was invalidated.

Table 2 shows the distance measurements obtained in the tests.

Taking the arithmetic mean of the valid distances we obtain a distance of 2.05 mm, therefore, it is considered that the optimum height of the perimeter of the new intermediate body will be 2 mm. Finally, a new intermediate body is designed with Autodesk Inventor software.

Finally, we obtain a new intermediate body for the Swagelok® cell, which will be manufactured and tested to verify that it meets our expectations.

Once the improvements to the Swagelok® cell were established and designed (process shown in Fig. 10A and D), the new supercapacitor was designed. For this purpose, each of the parts that make up this new cell is described.

Firstly, the novelty is described, which breaks with the Swagelok® cell design of an intermediate body with two threaded parts and interchangeable electrodes by a new design that has a fixed body to which one of the current collectors is integrated without the possibility of removing one of the current collectors. This part is illustrated in the Fig. 11A.

These figures show how the current collector, and the activated carbon tablet tank are integrated, simplifying the task of inserting the tablets.

The Fig. 11B shows the mobile current collector, which has been considered as such for a fundamental reason with respect to the design of the Swagelok® cell, and that is that the collector itself now has a thread on its contour, which allows the materials inside the cell to fit perfectly without being able to fracture when pressure is exerted. It is essential that there is perfect contact between the current collectors and the materials, as justified by many authors in their articles, in which they incorporate springs in the cell so that the collectors exert the necessary pressure.

The last element that makes up this new cell design is the locking device of the system, which has two threads, a first one to allow adjusting the pressure of the current collector and a second one that allows threading into the body of the cell for its closure (Fig. 11C).

Finally, the Fig. 11D of the result of the cell designed with Autodesk Inventor is shown. Also, Fig. 12 shows the final result of the body insert in the newly designed Swagelok® cell.

For the fabrication of all the designs shown, different manufacturing methodologies and processes have been used. The fabrication method used to materialise the designed supercapacitor is fused deposition modelling.

An ender 3 Pro® 3D printer has been used to manufacture the new Swagelok® intermediate cell body.

3.4. Final evaluation of the supercapacitor. Electrochemical tests

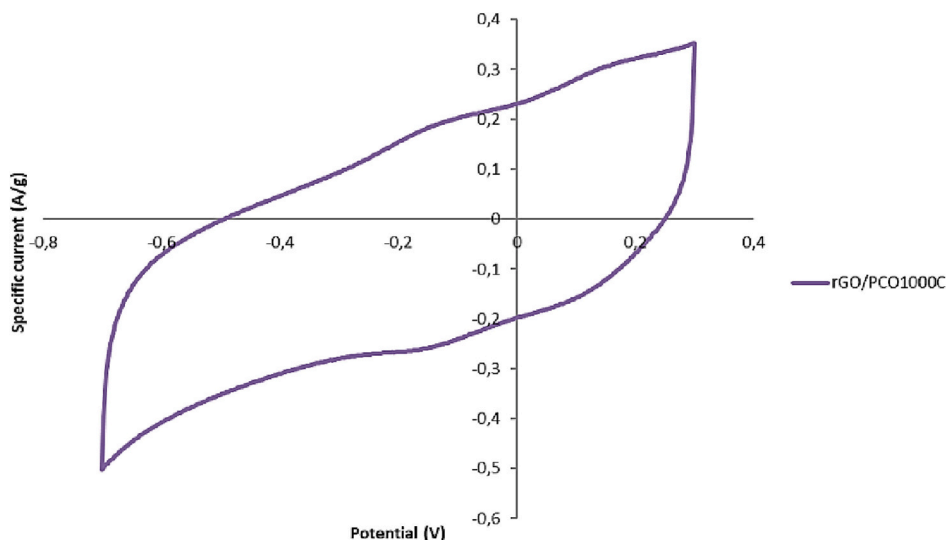In order to analyse the results obtained from the supercapacitors

Fig. 13. An example of a cyclic voltammetry test with the graphite collectors.
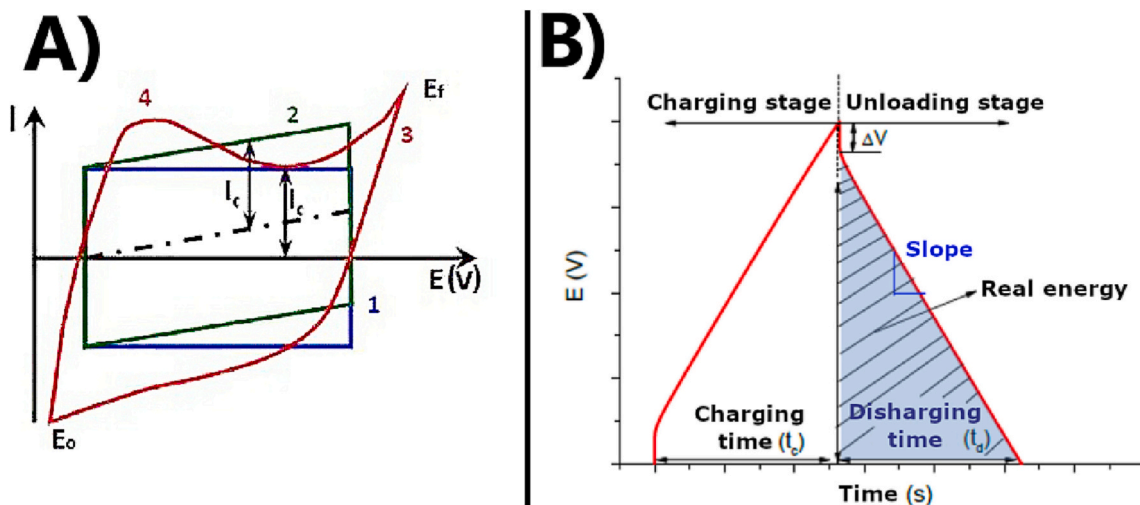
Fig. 14. A) Examples of cyclic voltammetry in supercapacitors. B) Example of charge-discharge profile for a super capacitor.

manufactured by means of the methodology proposed in this work, a series of tests are proposed to be carried out with a Potentiostat/Galvanostat (Autolab PGSTAT204). The main tests proposed are cyclic voltammetry and galvanostatic charge-discharge:

➢ Cyclic voltammetry:

It is one of the most important techniques in the field of electrochemistry (Fig. 13). It is based on the application of an electric potential perturbation in the form of a linear variation as a function of time and the recording of the response current. In order to avoid unwanted reactions in the electrolyte, the current potential range is limited between two preset values (E0 and Ef). In addition, it is also possible to adjust the voltage variation per unit time (sV/dt) [38,39].

The potentiostat-galvanostat applies a potential (E) and receives the signal of the current intensity (I), whose graph (result of the study) is called voltammogram.

Fig. 14A shows four graphs: the first one corresponds to an ideal capacitor (which does not exist in reality), the second one corresponds to a capacitor with resistance that is far from ideal. Finally, the red graph corresponds to a carbon capacitor where the electrolyte is decomposed, with peaks (point 4) due to the redox reactions and the formation of the electrical double layer.

By means of this test, we can determine whether the behaviour of the electrode is reversible in the potential range studied, which is calculated by means of the Coulombic efficiency (μ).

In capacitive materials, the criterion used to consider whether the process is reversible is defined by a coulombic efficiency higher than 95 %.

$$\mu(\%) = \frac{Q_c}{Q_a} \cdot 100 \Big) \tag{5}$$

where Qc and Qa correspond to the accumulated charge during the cathodic and anodic sweeps respectively.

The accumulated charge can be calculated from the sweep speed in cyclic voltammetry (s), the current recorded on the potentiostat during voltammetry (I) and the potential limits (E0 and Ef).

$$Q(C) = \int C \cdot dV = \frac{1}{S} \cdot \int_{E0}^{Ef} I \cdot dV \tag{6}$$

The capacitance of an electrode in farads is calculated by Eq. (7):

$$C(F) = \frac{\int_{E0}^{Ef} I \cdot dV}{S \cdot \Delta V} \tag{7}$$

where $\triangle$V is the range of potential in which you work (Ef – E0).

To calculate the specific capacitance (Cma) simply divide the electrode capacitance (C) by the grams of active electrode material (m).

$$C_{ma}\left(F \cdot g^{-1}\right) = \frac{C(F)}{m} \tag{8}$$

➢ Galvanostatic charge-discharge

The electrochemical technique of galvanostatic charging and discharging is based on the measurement of the potential of a system as a function of time, during the application of a constant current intensity (Fig. 14B). During the charging stage, a positive current is applied, while during the discharging stage, the sign of the current is changed, and a negative current is applied. The potentiostat measures the potential between the electrodes while the current is applied, resulting, in the case of a supercapacitor, in curves of potential (E) versus time (t).

The main parameters for assessing the functionality of the supercapacitor are [40–44]:

➢ Capacitance of the supercapacitor: The capacitance of the supercapacitor (Ccell) is obtained from the slope of the discharge curve.

$$C_{cell}\left(Fg^{-1}\right) = \left(\frac{I(A)}{slope_{discharge}(Vs^{-1}) \cdot m_{tma}}\right) \tag{9}$$

where I is the current (A) applied in the discharge and mtma is the mass of the active material of the two electrodes (mtma = m+ + m-).

➢ Capacitance of individual electrodes: A supercapacitor can be thought of as two capacitors connected in series. These capacitors are formed by the electrical double layer established between the electrode and the electrolyte ions.

$$\frac{1}{m_{tma} \cdot C_{cell}} = \frac{1}{m_+ \cdot C^+} + \frac{1}{m_- \cdot C^-} \tag{10}$$

where C+ and C- correspond to the capacitances (measured in Farads per gram) of the positive and negative electrode respectively.

➢ Equivalent series resistance: The equivalent series resistance (ESR) of the supercapacitor is obtained by dividing the ohmic drop observed at the start of the discharge ($\triangle$V) by the current variation to which it is subjected. Generally, the ESR is multiplied by the geometrical area of the electrode (A) to be expressed in $\Omega \cdot cm^2$.

Table 3

Carbonaceous systems used for the manufacture of electrodes and their electrical conductivity. The material listed first indicates that it is the major component of the mixture.

Samples	σ $(\Omega^{-1} \cdot m^1)$
PCO-1000C/graphite	123.00

$$ESR\left(\Omega * cm^2\right) = \frac{\Delta V}{2 \cdot I} \cdot A \tag{11}$$

➤ Actual specific energy: The actual specific energy (E_{real}) is obtained from the applied discharge current (I) divided by the total mass of the active material (mtma), multiplied by the area under the discharge curve.

$$E_{real}\left(kW \cdot kg^{-1}\right) = \frac{I}{m_{tma}} \cdot \int_{ti}^{tf} V \cdot dt \tag{12}$$

➤ Maximum energy: The maximum energy (E_{max}) can be obtained assuming an ideal behaviour of the supercapacitor, in which there is no ohmic drop and no deviations in the discharge curve.

$$E_{max}\left(kW \cdot kg^{-1}\right) = \frac{C \cdot V^2}{4 \cdot ESR} \tag{13}$$

➤ Average power: The average power (P_{med}) is calculated considering the actual energy, divided by the discharge time (td).

$$P_{mED}\left(kW \cdot kg^{-1}\right) = \frac{E_{real}}{t_d} \tag{14}$$

➤ Maximum power: In the same way as for maximum energy, a simplification is assumed to obtain the maximum power (P_{max}):

$$P_{max}\left(kW \cdot kg^{-1}\right) = \frac{V^2}{4 \cdot ESR} \tag{15}$$

3.5. Testing the validity of the proposed model

To validate the improved model, the results of a cyclic voltammetry test and a galvanostatic charge-discharge test on a supercapacitor are shown below, following the design and manufacturing guidelines for each of the elements that make up a supercapacitor.

Among the most commonly used materials in the manufacture of electrodes for supercapacitors are carbon-based electrodes.

To prove that the method proposed in this work is valid, the material PCO-1000C was used as an electrode material, a commercial activated carbon (supplied by GalaQuim) characterised by its porous structure, which leads to certain electrical conductivity properties, and natural gafite (supplied by Merck).

The physical characterisation of the carbons was assessed by the electrical conductivity of the electrodes prepared from them. The electrical conductivity of the materials is a very important property to take into account, as it can determine the suitability of an activated carbon as an electrode in a supercapacitor. The higher the conductivity, the greater its contribution to reducing the equivalent resistance of the system, and thus helping to reduce the power output of the cell.

The carbonaceous systems used to make the electrodes are shown in Table 3.

Fig. 15 represents the cyclic voltammograms of all samples at a sweep rate of 0.005 V s^{-1} using 1 M H2SO4 as the electrolyte for the four cells prepared.

The PCO-1000C/Graphite carbon system showed a quasi-rectangular voltammogram, typical of electrochemical double layer capacitors (EDL), with low diffusional restriction to the electrolyte.

Table 4 shows the values obtained by cyclic voltammetry. The coulombic efficiency was determined by the accumulated charge in the cathodic and anodic sweeps. The values obtained above 95 % indicate that the behaviour of the electrode is reversible. From the above table, it can be deduced that the sample has a high reversibility.

The galvanostatic charging and discharging technique consists of applying a continuous and constant current during a certain time interval until the potential limit set for the charge is reached. The ions then migrate to the surface of the electrodes and are stored there, at which point the system is said to be charged. However, if at any given moment the applied current is reversed for a period of time, the system will discharge, releasing energy. The representation of the potential values versus time shows the process of charging and discharging the system. For an ideal capacitor, the curve obtained should be perfectly triangular.

Fig. 16 plots the potential (V) versus time (t), and gives a linear response with a positive slope when charging the system, and a negative slope when discharging it. It is also observed that the supercapacitor shows an almost triangular shape, which again indicates that the example sample behaves almost like an ideal electrochemical double layer (EDL) with low resistance and good diffusion of the electrolyte

Table 4

Cyclic voltammetric properties of samples in 1 M H$_2$SO$_4$ at 0.005 V s^{-1}.

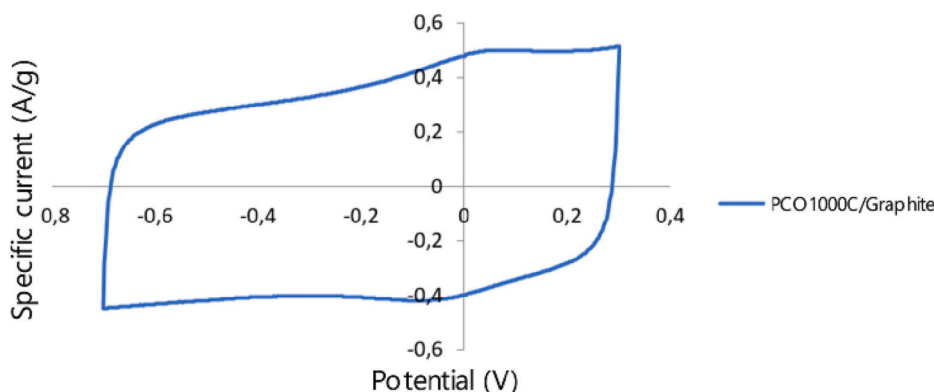| Samples	Total mass of electrodes (g)	Cycle area (A-s)	Specific capacity (F·g^{-1})	Coulombic efficiency μ (%)
PCO-1000C/graphite	1121.10	0.367	0.402	0.628

Fig. 15. Cyclic voltammetry in H$_2$SO$_4$ at 1 M at 0.005 V/s.
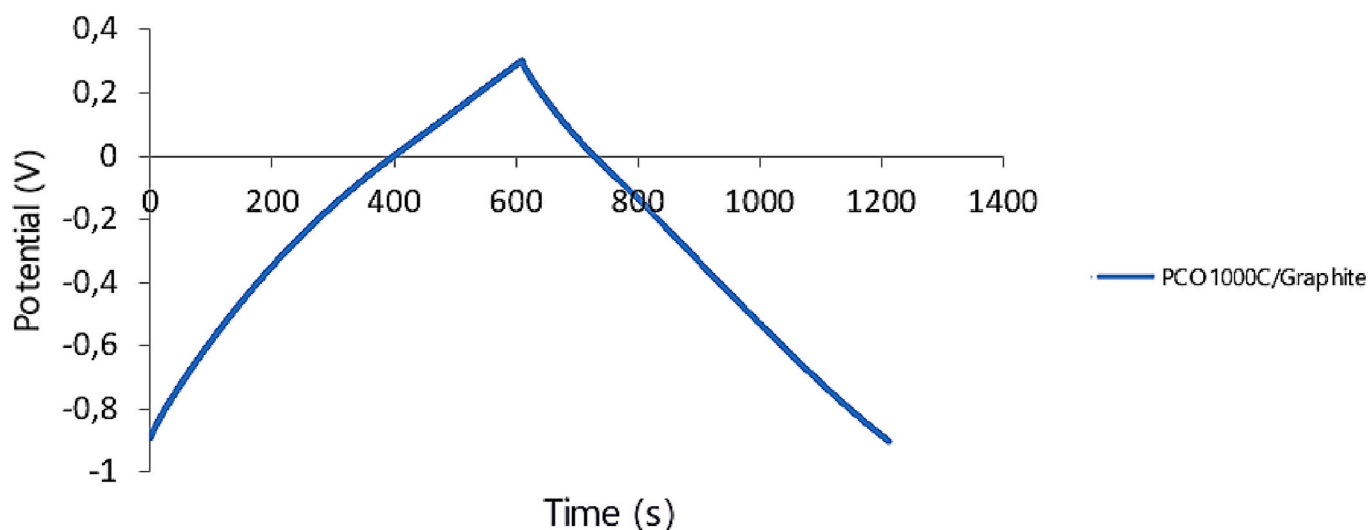
Fig. 16. Galvanostatic charge-discharge in H_2SO_4 at 1 M at 0.005 V/s and at a current load of 200 mA g^{-1}.

inside the pores.

In view of the results, a typical behaviour of electrochemical double layer (EDL) supercondensers is observed, validating the methodology proposed in this work.

4. Conclusions

The work presented here improves on the current state of the art. To this end, several conclusions have been reached:

➢ The process carried out to measure the parallelism of the collectors and consequently the number of contact points allows not only to validate the design followed in this work, but also all the designs based on the use of a fixed body (Swagelok® cell) comprising two or more collectors, several electrodes, and a separator.
➢ The collectors made of brass and copper were not valid as they suffered from aggressive oxidation processes and galvanic couples, so they could only be used a very limited number of times.
➢ The collectors made of graphite proved to be very effective against aggressive oxidation processes and galvanic couples and even these collectors, by releasing small amounts of material when rubbed, allow the complete cleaning of the collector faces, which improves the lifetime of the collectors.
➢ The design proposed for the creation of a new body to replace the traditional Swagelok® cell allows the thread to be limited and avoids breakage of the pads that act as electrodes, due to excessive threading of the device. To this end, an intermediate body was designed with an optimum height that never allows the thread to be used up until the entire thread is consumed. In addition, by integrating the current collector and the tank of the proposed design, the task of inserting the electrodes and their positioning is simplified.

CRediT authorship contribution statement

- AM contributed to conception and design of the study and wrote the first draft of the manuscript.
- JP contributed to conception and design of the study and organized the database.
- LM wrote sections of the manuscript and contributed to the experimental part.
- AC wrote sections of the manuscript and organized the database.
- JM contributed to the experimental part and wrote the definitive version of the manuscript.

The Author Contributions statement must describe the contributions of individual authors referred to by their initials and, in doing so, all authors agree to be accountable for the content of the work.

Jesús M. Rodríguez-Rego: Investigation and Writing – Original Draft.
Laura Mendoza-Cerezo: Investigation and Writing – Original Draft.
Juan Pablo Carrasco-Amador: Supervision and validation.
Alfonso Carlos Marcos-Romero: Supervision and validation.
A. Macías-García: conceptualization and Review & Editing.

Declaration of competing interest

The authors declare that the research was conducted in the absence of any commercial or financial relationships that could be construed as a potential conflict of interest.

Data availability

Data will be made available on request.

References

[1] I.G. Zúñiga Santiz, Estudio de las densidades de estados de trampas en celdas solares de kesterita, por medio de la simulación en AMPS-1D, in: Exploraciones, intercambios y relaciones entre el diseño y la tecnología, 2020, pp. 57–79, doi: 10.16/CSS/JQUERY.DATATABLES.MIN.CSS.
[2] D. M. Pasquevich, "Asociación Argentina para el Progreso de las Ciencias (AAPC)," La creciente demanda mundial de energía frente a los riesgos ambientales. https://aargentinapciencias.org/grandes-temas-ambientales/energia-y-ambiente-3/ (accessed Dec. 28, 2022).
[3] 2020 climate & energy package. https://climate.ec.europa.eu/eu-action/climate-strategies-targets/2020-climate-energy-package_en. (Accessed 26 December 2022).
[4] J. K. Kaldellis and D. Zafirakis, "Optimum energy storage techniques for the improvement of renewable energy sources-based electricity generation economic efficiency," Energy, vol. 32, no. 12, pp. 2295–2305, Dec. 2007, doi:https://doi.org/10.1016/J.ENERGY.2007.07.009.
[5] R. Baños, F. Manzano-Agugliaro, F. G. Montoya, C. Gil, A. Alcayde, and J. Gómez, "Optimization methods applied to renewable and sustainable energy: a review," Renew. Sust. Energ. Rev., vol. 15, no. 4, pp. 1753–1766, May 2011, doi:https://doi.org/10.1016/J.RSER.2010.12.008.
[6] M. Winter and R. J. Brodd, "What are batteries, fuel cells, and supercapacitors?," Chem. Rev., vol. 104, no. 10, pp. 4245–4269, Oct. 2004, doi:https://doi.org/10.1021/CR020730K/ASSET/IMAGES/MEDIUM/CR020730KE00045.GIF.
[7] J. Yang, M. A. Bissett, and R. A. W. Dryfe, "Investigation of voltage range and self-discharge in aqueous zinc-ion hybrid supercapacitors," ChemSusChem, vol. 14, no. 7, p. 1700, Apr. 2021, doi:https://doi.org/10.1002/CSSC.202002931.
[8] W. Zuo et al., "Battery-supercapacitor hybrid devices: recent Progress and future prospects," Adv. Sci., vol. 4, no. 7, p. 1600539, Jul. 2017, doi:https://doi.org/10.1002/ADVS.201600539.
[9] M. Armand and J. M. Tarascon, "Building better batteries," Nature, vol. 451, no. 7179, pp. 652–657, Feb. 2008, doi:https://doi.org/10.1038/451652a.
[10] C. Valdivia Miranda, Impresoras 3D: el futuro del modelado, 2020.

[11] M. González, Potenciostato | La Guía de Química, Nov. 19 (2010). https://quimica.laguia2000.com/conceptos-basicos/potenciostato. (Accessed 30 December 2022).

[12] Ultimaker Cura|Ultimaker. https://ultimaker.com/es/software/ultimaker-cura. (Accessed 30 December 2022).

[13] Software Inventor|Autodesk. https://www.autodesk.es/products/inventor/overview?term=1-YEAR&tab=subscription&plc=INVPROSA. (Accessed 28 December 2022).

[14] Inventor Software|Autodesk. https://www.autodesk.com/products/inventor/overview?term=1-YEAR&tab=subscription. (Accessed 26 December 2022).

[15] Software de AutoCAD|Autodesk. https://www.autodesk.es/products/autocad/. (Accessed 28 December 2022).

[16] 3-D Printing Methods|Ceramic Industry. http://www.ceramicindustry.com/articles/91971-3-d-printing-methods/. (Accessed 26 December 2022).

[17] A. G. Pandolfo and A. F. Hollenkamp, "Carbon properties and their role in supercapacitors," J. Power Sources, vol. 157, no. 1, pp. 11–27, Jun. 2006, doi:https://doi.org/10.1016/J.JPOWSOUR.2006.02.065.

[18] I. Aldama, Electrodos para supercondensadores obtenidos por electrodeposición, Universidad Autónoma de Madrid, Madrid, 2015.

[19] B. E. Conway and W. G. Pell, "Double-layer and pseudocapacitance types of electrochemical capacitors and their applications to the development of hybrid devices," J. Solid State Electrochem., vol. 7, no. 9, pp. 637–644, Sep. 2003, doi:https://doi.org/10.1007/S10008-003-0395-7.

[20] T. A. Centeno and F. Stoeckli, "The role of textural characteristics and oxygen-containing surface groups in the supercapacitor performances of activated carbons," Electrochim. Acta, vol. 52, no. 2, pp. 560–566, Oct. 2006, doi:https://doi.org/10.1016/J.ELECTACTA.2006.05.035.

[21] E. Frackowiak, G. Lota, J. Machnikowski, C. Vix-Guterl, and F. Béguin, "Optimisation of supercapacitors using carbons with controlled nanotexture and nitrogen content," Electrochim. Acta, vol. 51, no. 11, pp. 2209–2214, Feb. 2006, doi:https://doi.org/10.1016/J.ELECTACTA.2005.04.080.

[22] N. L. Wu, "Nanocrystalline oxide supercapacitors," Mater. Chem. Phys., vol. 75, no. 1–3, pp. 6–11, Apr. 2002, doi:https://doi.org/10.1016/S0254-0584(02)00022-6.

[23] G. A. Snook, P. Kao, A. S. Best, G. A. Snook, P. Kao, and A. S. Best, "Conducting-polymer-based supercapacitor devices and electrodes," JPS, vol. 196, no. 1, pp. 1–12, Jan. 2011, doi:https://doi.org/10.1016/J.JPOWSOUR.2010.06.084.

[24] F. Béguin, M. Friebe, K. Jurewicz, C. Vix-Guterl, J. Dentzer, and E. Frackowiak, "State of hydrogen electrochemically stored using nanoporous carbons as negative electrode materials in an aqueous medium," Carbon NY, vol. 44, no. 12, pp. 2392–2398, Oct. 2006, doi:https://doi.org/10.1016/J.CARBON.2006.05.025.

[25] S.T. Aziz, S. Kumar, S. Riyajuddin, K. Ghosh, G.D. Nessim, D.P. Dubal, Bimetallic phosphides for hybrid supercapacitors, J. Phys. Chem. Lett. 12 (2021) 5138–5149, https://doi.org/10.1021/ACS.JPCLETT.1C00562/ASSET/IMAGES/MEDIUM/JZ1C00562_0005.GIF.

[26] P. Díaz, Supercondensadores híbridos asimétricos con especies redox inorgánicas, Universidad de Oviedo, Oviedo, 2016. Accessed: Dec. 26, 2022. [Online]. Available: https://digibuo.uniovi.es/dspace/handle/10651/40605.

[27] S. Roldán, M. Granda, R. Menéndez, R. Santamaría, and C. Blanco, "Mechanisms of energy storage in carbon-based supercapacitors modified with a quinoid redox-active electrolyte," J. Phys. Chem. C, vol. 115, no. 35, pp. 17606–17611, Sep. 2011, doi:https://doi.org/10.1021/JP205100V/ASSET/IMAGES/MEDIUM/JP-2011-05100V_0003.GIF.

[28] B.E. Conway, Electrochemical Supercapacitors: Scientific Fundamentals and Technological Applications, Springer Science & Business, 1999.

[29] C. Moreno-Castilla, F. Carrasco-Marín, and A. Mueden, "The creation of acid carbon surfaces by treatment with (NH4)2S2O8," Carbon NY, vol. 35, no. 10–11, pp. 1619–1626, Jan. 1997, doi:https://doi.org/10.1016/S0008-6223(97)00121-8.

[30] J. Pastor-Villegas, C. Valenzuela-Calahorro, A. Bernalte-Garcia, and V. Gomez-Serrano, "Characterization study of char and activated carbon prepared from raw and extracted rockrose," Carbon NY, vol. 31, no. 7, pp. 1061–1069, Jan. 1993, doi:https://doi.org/10.1016/0008-6223(93)90057-H.

[31] V. Gómez-Serrano, E. M. Cuerda-Correa, M. C. Fernández-González, M. F. Alexandre-Franco, and A. Macías-García, "Preparation of activated carbons from chestnut wood by phosphoric acid-chemical activation. Study of microporosity and fractal dimension," Mater. Lett., vol. 59, no. 7, pp. 846–853, Mar. 2005, doi:https://doi.org/10.1016/J.MATLET.2004.10.064.

[32] M. Jagtoyen and F. Derbyshire, "Some considerations of the origins of porosity in carbons from chemically activated wood," Carbon NY, vol. 31, no. 7, pp. 1185–1192, Jan. 1993, doi:https://doi.org/10.1016/0008-6223(93)90071-H.

[33] C. J. van Oss, "A review of: 'active carbon.'," J. Dispers. Sci. Technol., vol. 11, no. 3, pp. 323–323, Jun. 1990, doi:https://doi.org/10.1080/01932699008943255.

[34] F. Rodríguez-Reinoso and M. Molina-Sabio, "Activated carbons from lignocellulosic materials by chemical and/or physical activation: an overview," Carbon NY, vol. 30, no. 7, pp. 1111–1118, Jan. 1992, doi:https://doi.org/10.1016/0008-6223(92)90143-K.

[35] J. Yang, M. A. Bissett, and R. A. W. Dryfe, "Investigation of voltage range and self-discharge in aqueous zinc-ion hybrid supercapacitors," ChemSusChem, vol. 14, no. 7, p. 1700, Apr. 2021, doi:https://doi.org/10.1002/CSSC.202002931.

[36] V. Ruiz, C. Blanco, E. Raymundo-Piñero, V. Khomenko, F. Béguin, and R. Santamaría, "Effects of thermal treatment of activated carbon on the electrochemical behaviour in supercapacitors," Electrochim. Acta, vol. 52, no. 15, pp. 4969–4973, Apr. 2007, doi:https://doi.org/10.1016/J.ELECTACTA.2007.01.071.

[37] A. Burke, "Ultracapacitors: why, how, and where is the technology," J. Power Sources, vol. 91, no. 1, pp. 37–50, Nov. 2000, doi:https://doi.org/10.1016/S0378-7753(00)00485-7.

[38] R. González, B. Xochiquetzal, A. Reyes, Estudio electroquímico por voltamperometría cíclica del glutatión oxidado y reducido, Revista Cubana de Química 17 (1) (2005) 22.

[39] I. G. Meza-Pardo et al., "Synthesis of UV-11 MOF and its characterization by cyclic voltammetry," Front Chem, vol. 8, p. 617, Aug. 2020, doi:https://doi.org/10.3389/FCHEM.2020.00617.

[40] J. van Herpt Valdivia, Implementación de un sistema de medida de capacidad de carga para caracterizar materiales que se puedan comportar como supercondensadores, Universitat Politècnica de València, Alcoi, 2016. Accessed: Dec. 30, 2022. [Online]. Available: https://riunet.upv.es/bitstream/handle/10251/73888/HERPT%20-%20Implementaci%C3%B3n%20de%20un%20sistema%20de%20medida%20de%20capacidad%20de%20carga%20para%20caracterizar%20materiales....pdf?sequence=2.

[41] M. Prieto Lobato, Diseño de materiales de carbono bioderivados. Aplicación como electrodos en condensadores electroquímicos, Universidad Politécnica de Madrid, Madrid, 2019. Accessed: Dec. 30, 2022. [Online]. Available: https://oa.upm.es/55972/1/TFM_MANUEL_PRIETO_LOBATO.pdf.

[42] S. Gómez-Biedma, E. Soria, M. Vivó, Análisis electroquímico, Revista de Diagnóstico Biológico vol. 51 (1) (2002) 18–27. Accessed: Dec. 30, 2022. [Online]. Available: https://scielo.isciii.es/scielo.php?script=sci_arttext&pid=S0034-79732002000100005&lng=es&nrm=iso&tlng=es.

[43] C. Yun and S. Hwang, "Analysis of the charging current in cyclic voltammetry and supercapacitor's galvanostatic charging profile based on a constant-phase element," ACS Omega, vol. 6, no. 1, pp. 367–373, Jan. 2020, doi:https://doi.org/10.1021/ACSOMEGA.0C04702.

[44] M. Fukuhara, K. Sugawara, Electric charging/discharging characteristics of super capacitor, using de-alloying and anodic oxidized Ti-Ni-Si amorphous alloy ribbons, Nanoscale Res. Lett. 9 (1) (2014) 1–6, https://doi.org/10.1186/1556-276X-9-253.

[45] CO2: emisiones mundiales 1995--2021|Statista, Emisiones mundiales de CO2 de 1995 a 2021. https://es.statista.com/estadisticas/635894/emisiones-mundiales-de-dioxido-de-carbono/, Feb. 24, 2022. (Accessed 30 December 2022).

[46] A. G. Pandolfo and A. F. Hollenkamp, "Carbon properties and their role in supercapacitors," J. Power Sources, vol. 157, no. 1, pp. 11–27, Jun. 2006, doi:https://doi.org/10.1016/J.JPOWSOUR.2006.02.065.